Novel Electrical Joints Using Deformation Machining Technology Part I: Computer Modeling

Lyudmila Solovyeva, Nikolay Zubkov, Bohdan Lisowsky, and Alaa Elmoursi

***Abstract*— This paper explores the use of deformation machining technology (DMT), originally developed at Bauman Moscow State Technical University, to make electrical joints and compare their performance to bolted and welded electrical joints. The DMT process is used to generate tooth-like profiles on two opposing surfaces that make the electrical joint, which are later joined by applying a mechanical load. To optimize the interfacing surface tooth-like profiles, a computational finite element model is developed. The model is used to simulate the mechanical joining of both Cu and Al DMT joints. The model is able to predict the most important parameters that contribute to enhancing the teeth interlocking and increasing the contact surface area. The model is successfully used in optimizing Cu-DMT joints; however, for Al-DMT joints the model predicted an unreliable electrical joint attributed to a spring-back effect that occurs after the mechanical load for making the joint is removed.**

***Index Terms*— Deformation angle, deformation machining, filling, locking interference, modeling, slenderness ratio, spring back, tooth geometry.**

I. Introduction

ELECTRICAL joints for high-current applications (current carrying capacity for Cu-10A/mm^2; for Al-7A/mm^2) are typically made using bolting, welding, brazing, and swaging [1], [2]. This paper explores a novel joining technology for making electrical joints using deformation machining technology (DMT). DMT is based on using a specially-designed cutting tool [3] that undercuts and lifts (mechanically deforms) the machined surface to form a tooth-like structure, such as shown in Fig. 1. The DMT process can be applied to flat surfaces as well as cylindrical surfaces, also shown in Fig. 1. The literature reports of using this technology for multiple applications, such as thermal management, electrical joints, filters, frictional surfaces, and others [4]–[7].

This paper explores the use of DMT technology to fabricate electrical joints made using Cu and Al materials. Successful implementation of DMT electrical joints for high-current carrying structures (exceeding 100 A) could possibly provide maintenance-free electrical enclosures, by displacing bolted joints. The integrity of the DMT joints will be assessed through computational modeling; the modeling is expected to enable the optimization of the DMT profile and the selection of suitable mechanical joining load required to achieve best electrical and mechanical performance. In a later paper, we use the optimized DMT profile to prepare experimental DMT joints of Cu and Al, and compare their performance to bolted and welded joints.

Manuscript received December 22, 2011; revised May 10, 2012; accepted June 30, 2012. Date of publication August 31, 2012; date of current version September 28, 2012. Recommended for publication by Associate Editor W. D. Brown upon evaluation of reviewers' comments.

L. Solovyeva and A. Elmoursi are with the Eaton Innovation Center, Eaton Corporation, Southfield, MI 48076 USA (e-mail: LyudmilaSolovyeva@eaton.com; AlaaAElmoursi@eaton.com).

N. Zubkov is with Bauman Moscow State Technical University, Moscow 10505, Russia (e-mail: zoubkovn@bmstu.ru).

B. Lisowsky is with Materials Technology, Troy, MI 48084 USA (e-mail: lisowsky@bohdan.cnc.net).

Color versions of one or more of the figures in this paper are available online at http://ieeexplore.ieee.org.

Digital Object Identifier 10.1109/TCPMT.2012.2207723

II. Fabricating a DMT Electrical Joint

In this paper, we examined two electrical geometries: a lap joint and an edge joint; both are typically used in high-current applications. Fig. 2 shows the lap joint with the DMT along the flat surface of the bar. Fig. 3 shows the edge joint with the DMT profiled across the thickness of the bar.

There are some key considerations regarding DMT as it applies to joints.

1) Tooth geometry can be quite variable in dimensions of tooth height, tooth spacing (pitch), and tooth thickness. A parameter of "slenderness ratio," a ratio of tooth height to tooth thickness, is a characteristic used in evaluation of the impact of different geometries on joint characteristics. Fig. 4 shows tooth geometries that could affect electrical joints. The tooth width and the groove width can be a variable based on the capabilities of fin generation and assembly equipment, which would allow easy engagement prior to force application and, which would allow for automated assembly. The incomplete fin formation at the start of DMT needs to be considered during joint design to assure joint strength and conductivity.
2) Incomplete tooth formation at the start of fin cutting, as observed in Fig. 4(b), is a result of unavailable material to form a complete tooth. This phenomenon cannot be corrected and must be accounted for in the joint design.
3) Tooth forward deformation is a characteristic of the DMT process, and is created by the tool force and friction between the tool and the material during the DMT process. This phenomenon can only be partially corrected on the tool exit side by initial chamfering of the plate in the amount of tooth overhang. However, this is not practical for materials thinner than about 6 mm as the forward lean takes away from the tooth engagement area for DMT joints. This can be observed in Fig. 5

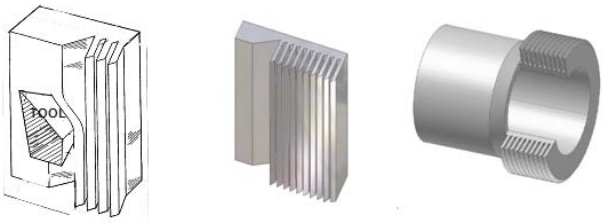

Fig. 1. Principle of (a) DMT and (b) schematics of flat and cylindrical DMT surfaces.

Fig. 2. Lap joint showing the DMT profile on the flat surface of the bar 20 mm wide and 4 mm thick.

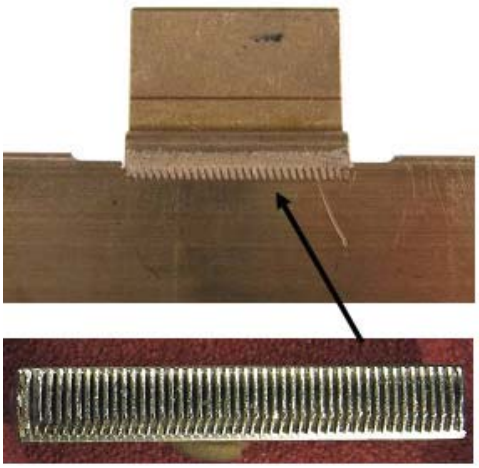

Fig. 3. Edge joint with the DMT profile across the 6.35-mm thickness of the bar.

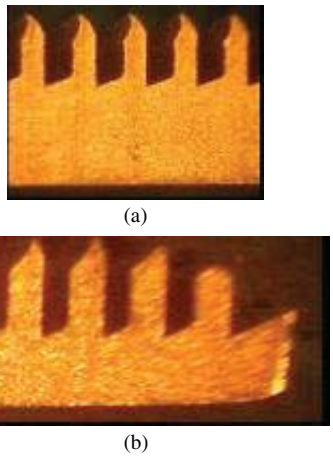

Fig. 4. DMT profiles used for joint evaluation. (a) Similar geometry to M-Cu-1 with slenderness ratio of 3.33. (b) Geometry with interference fit with aspect ratio of 3.5% and 18% interference.

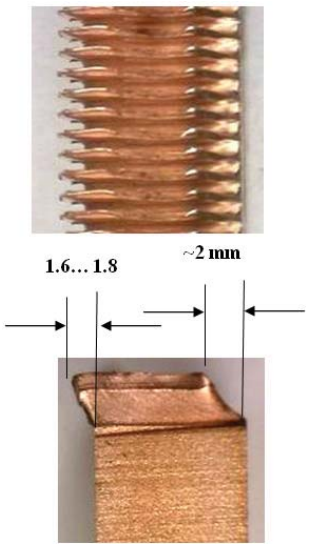

Fig. 5. Forward DMT tooth deformation on 6.35 mm thick copper plate. Tool motion is from right to left.

where a DMT profile was generated on 6.35 mm thick copper plate, and it shows a forward deformation of 2 mm and an overhang of 1.8 mm.

4) Proper orientation of opposing teeth prior to joining is critical so that the tooth tip is in contact with the incline at the opposing root. This orientation causes the teeth to slide down the root ramp, generate a curvature, and if there is a gap between the teeth, to initially upset the tooth thus creating a jigsaw-puzzle locking feature, which would be important for permanent joints.

III. Modeling DMT Electrical Joint

Modeling of electrical joints for strength and reliability has been done in bolted and welded joints [8], [9]. To develop a finite element model for DMT fin deformation, the DMT geometry was defined, and a reasonable approximation utilizing standard machined teeth was developed to quickly generate and assess the accuracy of the model under specific conditions. Although there are some differences between the standard machined and DMT profiles, as shown in Fig. 6, the machined approximation proved to be sufficient for assessing and understanding the effect of different parameters on the joint geometry. In addition, the model, developed using standard ANSYS 11 classic software 2-D [10], required large plastic deformation capability to accommodate modeling of tooth deformation under various constraints and loads.

The nomenclature for the DMT simplified profile is shown in Fig. 7 with the parameter nomenclature as shown in Table I for modeling of lap joints. Mechanical properties for the specific alloys used were experimentally measured, and are reported in Table II. We used homogeneous material properties (annealed Cu and solution heat treated Al), since DMT and machining processes have negligible cold work effect.

TABLE I

TOOTH PROFILE VARIATIONS AND ASSEMBLY LOADS FOR MACHINED COPPER AND ALUMINUM PLATES USED FOR COMPUTER MODELING

DMT parameter	Dimension	Units	Profile variation						
			M-Cu1	M-CuA12	M-Cu2	M-Cu3	M-Cu4	M-Cu5	M-CA1
Joint length	**L**	mm	20	20	20	20	20	20	20
Joint width	**D**	mm	20	20	20	20	20	20	20
Tooth pitch	**P**	mm	1.28	1.28	1.28	1.28	1.28	1.28	1.27
Groove width	**w**	mm	0.73	0.73	0.73	0.73	0.73	0.73	0.75
Tooth height	**h**	mm	1.83	1.83	1.83	1.83	1.33	1.33	1.88
Tooth angle	θ	degrees	90	90	90	90	90	90	90
Tooth tip angle	α	degrees	45	45	50	45	45	45	45
Root angle	β	degrees	45	45	45	45	45	30	45
Tooth width	**Ref**	mm	0.55	0.55	0.55	0.55	0.55	0.55	0.52
Assembly load		M-tons	17	10	17	17	17	17	10
Slenderness ratio	h/tooth width		3.33	3.33	3.33	3.33	2.42	2.42	3.62

Note: For M-Cu3, the angle θ for top plate is 100° and for bottom plate it is 80°. Aluminum assembly load changed to 10 tons.

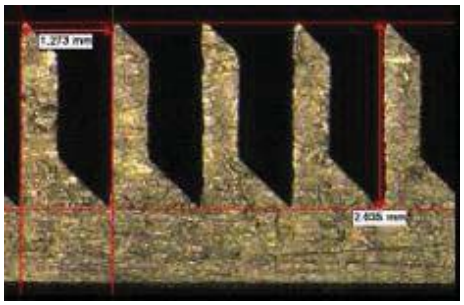

(a)

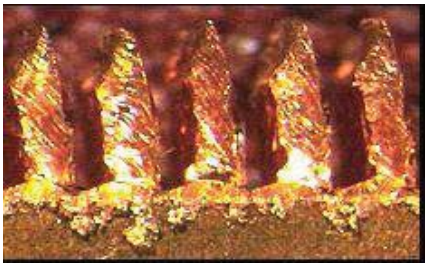

(b)

Fig. 6. (a) Machined DMT-like profile and (b) actual DMT profile.

TABLE II

APPROXIMATIONS OF TRUE STRESS-STRAIN PROPERTIES FOR COPPER AND ALUMINUM ALLOY 6101-T651

Property	Units	Copper	Aluminum
Elastic modulus	GPa	117.211	70.326
Tensile strength	MPa	238.5	159.0
Yield strength	MPa	185.0	116.5
Elongation	%	47	18
Poisson's ratio	–	0.33	0.33

The fin contact (before deformation) was an area contact. Sharp corners (singularity) were eliminated by flattening. The initial algorithm we used caused a lot of deformation at the tips of the fins. At that time, we used a friction coefficient of 1.00.

We changed the algorithm friction condition (coefficient of friction) to allow fin tip to slide to the bottom of the groove while bending and before any fin upsetting takes place. This was based on our experimental observations. We changed the friction coefficient to 0.1 but still had difficulties with the fins from the bottom plate. By changing the top surface rigidity, we were able to get proper deformation. We again changed the friction coefficient to 0.3 and used rigid top and bottom surfaces achieving proper fin deformation. This was the final contact condition, at least for the copper joints.

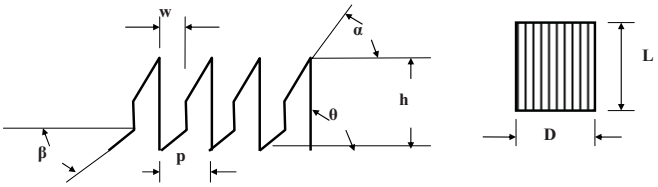

Fig. 7. Parameter nomenclature for DMT profile used in computer modeling.

Initially, the mesh elements were distorted beyond their limit at only 44% of the load. Then, we refined the mesh further and also changed friction coefficient to have the model accommodate the full load without excessive element distortion.

All copper, M-Al, and M-Al2 models had the same constraints as shown in Fig. 8, which represent lap joint geometry. There is a uniform pressure on the top surface, and the bottom surface is fixed. Note that there is no lateral constraint. Also, the friction between the tooth tip and the tooth root ramp was set at 0.3 to allow smooth tooth sliding during deformation as observed in experiments. Automatic meshing was done to properly track deformation and establish certain measurements on finished modeled joints.

The assembly forces were determined experimentally to avoid deformation of the plates and applied to the model. For copper, that force was 17 metric tons and for aluminum it was 10 metric tons as noted in Table I. A majority of the modeling focused on copper with variations of tooth height, tooth width, and tip and root angles to determine the degree of fin upset, which enhances locking of the fins. The width and height can be combined into a ratio, which was

TABLE III
MEASUREMENTS OF JOINT PARAMETERS FOR MODELED JOINTS

Model	Deformation angle	Tooth thickness		Locking interference	Root to root height	Joint height
		Ft	Ft			
	(degrees)	(mm)	(mm)	(mm)	(mm)	(mm)
M-Cu1	23.85	0.687	0.613	0.074	2.31	2.044
M-Cu2	17.13	0.672	0.629	0.043	2.15	2.026
M-Cu3	N/A	0.559	0.554	0.005	2.51	2.079
M-Cu4	19.01	0.702	0.623	0.079	1.83	1.707
M-Cu5	15.91	0.706	0.628	0.078	1.41	1.356
M-A12	26.87	0.644	0.591	0.053	2.37	2.765
M-A1	25.16	0.638	0.6	0.038	2.28	2.082

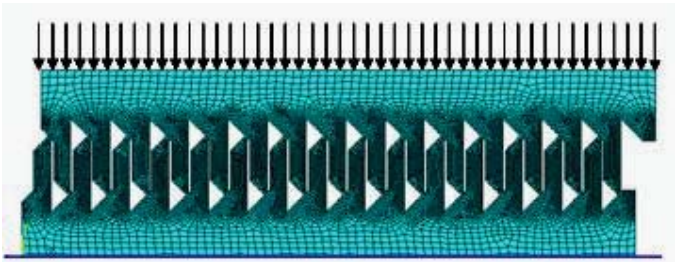

Fig. 8. Orientation and constraints of simulated DMT geometries prior to assembly.

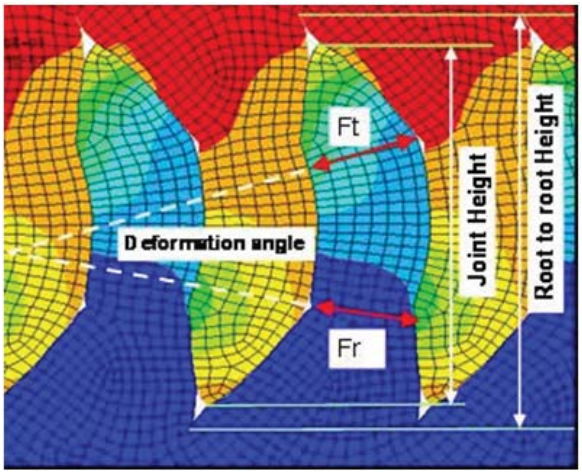

Fig. 9. Finished joint parameters developed during modeling.

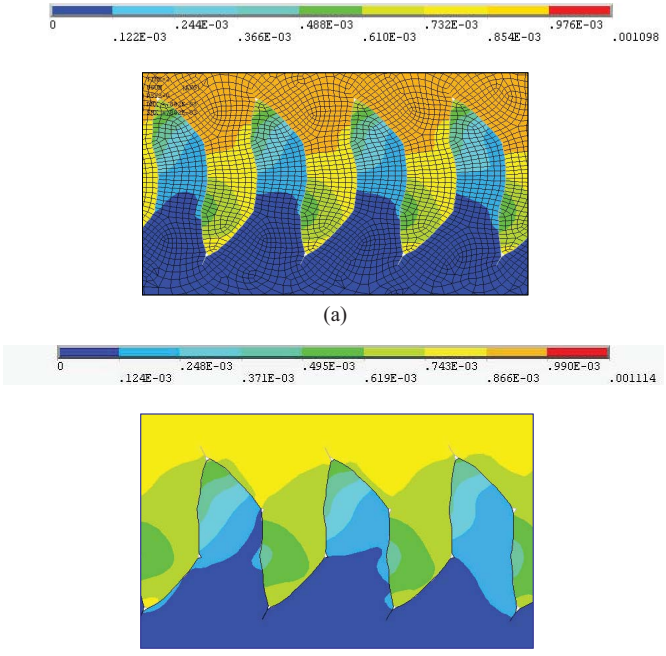

Fig. 10. Total deformation of (a) M-Cu1 and (b) M-Cu4 showing the effect of slenderness ratio on joint geometry.

termed as a "slenderness ratio." For permanent joints, which were of primary interest in this paper, tooth tip upsetting and the resulting interlocking along with deformation angle are important. Tooth interlocking is defined as the difference between the tooth thickness near the top of the tooth and the tooth thickness at the root, as shown in Fig. 9. Various other joint parameters were developed as a result of modeling and they are graphically defined in Fig. 9 with values shown in Table III.

It is observed that for copper, the most attractive model is that of M-Cu1 due to the favorable combination of deformation angle and the locking interference in addition to the complete contact of teeth from joined bars. In model M-Cu2, where the tip angle is different from the root angle, the deformation angle is much reduced along with the locking interference. Model M-Cu3 does not generate a joint curvature of the teeth since the mating teeth are already at 80° and 100°, and are flattened by the assembly forces without any upsetting of teeth. Because of that effect, the permutation of the effect of tooth angle was modeled only once as the fabrication of such mating geometries and assembly would be much more expensive needing two sets of fine machine tools, and there was no value of that permutation to pursue other off-90° fin angle permutations. Therefore, all other parameter permutations have the fin angle of 90°. For models M-Cu4 and M-Cu5, where the slenderness ratio is reduced from that of M-Cu1, there is a slightly greater tooth upsetting as evidenced by greater locking interference, but the deformation angle is much

TABLE IV
ADDITIONAL ALUMINUM GEOMETRIES AND MODEL BOUNDARY CONDITIONS EVALUATED TO IMPROVE JOINT SOUNDNESS

DMT parameter	Dimension	Units	Profile variation				
			M-A12	M-A13	M-A14	M-A14	M-Al5
Joint length	**L**	mm	20	20	20	20	20
Joint width	**D**	mm	20	20	20	20	20
Tooth pitch	**P**	mm	1.28	1.28	1.28	1.28	1.28
Groove width	**w**	mm	0.73	0.73	0.73	0.73	0.73
Tooth height	**h**	mm	1.83	1.83	1.83	1.83	1.83
Tooth angle	θ	degrees	90	90	90	90	90
Tooth tip angle	α	degrees	45	45	45	45	45
Root angle	β	degrees	45	45	45	45	45
Tooth width	**Ref**	mm	0.55	0.55	0.55	0.55	0.55
Assembly load		M-tons	10	10	11	10	10
Slenderness ratio	h/tooth width		3.33	3.33	3.33	3.33	3.33

Notes: M-Al2 - Same as M-Cu1.

M-Al3 - Same as M-AL2 with added lateral constraint on bottom plate

M-Al4 - Same as M-Al3 but assembled at 11 metric tons force.

M-Al5 - Same as M-Al3 with fixed top plate.

M-Al6 - Same as M-Al5, no lateral constraint, extra teeth on lower plate.

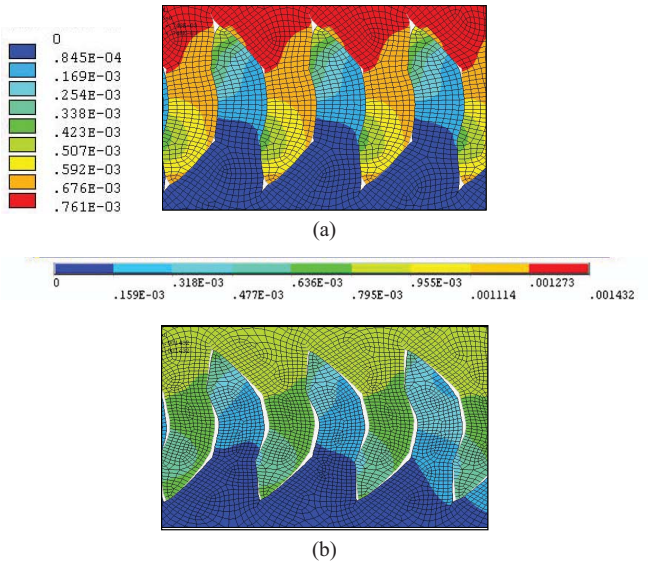

Fig. 11. Incomplete joint contact at the tooth tips in M-Al2 having the same geometry as (a) M-Cu1 and (b) incomplete contact in M-Al showing the effect of groove/fin gap and spring-back due to lower elastic modulus of aluminum.

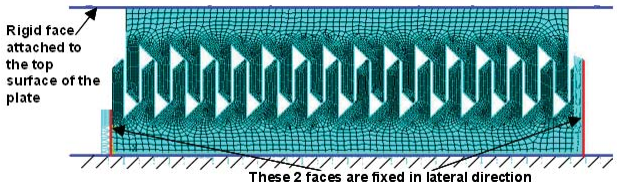

Fig. 12. Boundary conditions used for M-Al-3 and M-Al4 by adding lateral constraints and for M-Al5 by further adding the rigid top face/plate.

reduced. The effect of that slenderness ratio on joint geometry is shown in Fig. 10 for copper. Note that deformation units are in meters in Figs. 10 and 11.

The simulations for copper, regardless of tooth geometry clearly showed complete intimate contact between the teeth of the mating plates. However for aluminum, there is incomplete contact for the two permutations described in Table I. Table III shows that the amount of interlocking for M-Al2 and M-Al is much lower than for M-Cu1, which is the most attractive geometry for copper as stated above. However, the deformation angle for both aluminum geometries is larger than for M-Cu1 indicting that the DMT aluminum joint may have sufficient strength. On the other hand, there is significant amount of spring-back due to lower modulus of elasticity for aluminum, and this DMT mechanical joint does not appear to be as good electrically and environmentally as that for copper. Fig. 11 shows the appearance of tooth/groove gap on the aluminum joint. Because the tooth upsetting does not take place as readily as it does in copper, the gap between the mating teeth is not filled by plastic deformation, and spring-back is more clearly observed. This effect is critical to the joint soundness and also impacts gap tolerance.

In the effort to improve the aluminum joint, additional models were generated as shown in Table IV. All of the geometries are identical to M-Al2 (which is identical to M-Cu1) but the boundary conditions were changed as shown in Fig. 12 and further identified in the notes below Table IV. In one case, M-Al4, the assembly load was increased by 10%.

For model M-Al3, the effect of adding lateral constraint to the lower plate resulted in an inferior joint to that obtained in M-Al2 showing less filling of grooves, less interlocking, and

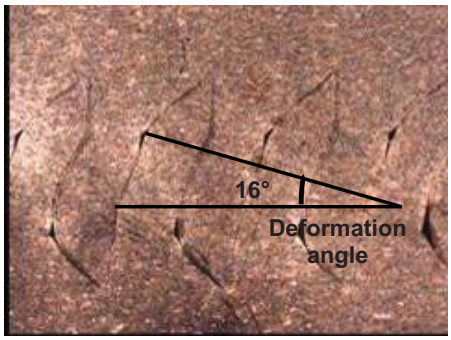

(a)

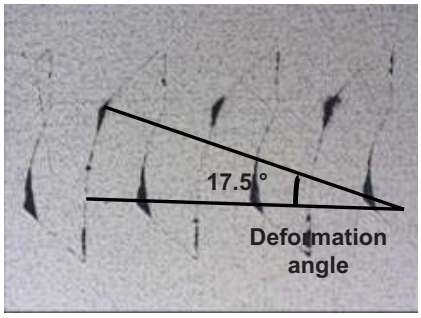

(b)

Fig. 13. Experimental results for joining (a) copper and (b) aluminum.

smaller joint angle. Increasing the load to 11 tons in the model M-Al4 and maintaining the lateral constraint on the lower plate brought the joint to the same deformation appearance as M-Al2, but that constraint reduces both the deformation angle and the amount of interlocking. In addition, that increased assembly load causes the joint to bulge laterally. All these effects make the model M-Al4 unacceptable. Changing the constraint on the top plate from uniform pressure to rigid plate with centrally located assembly load generated very similar results to M-Al2, thus providing an option for the assembly to be either done with uniform pressure or rigid plate centrally loaded. When lateral constraint on the bottom plate was replaced with additional teeth on each side of the upper plate, the deformation angle was reduced but the interlocking was reduced to that of M-Al3 and lacked full groove filling.

To verify that the model was generating acceptable results, actual geometries of M-Cu1 and M-Al were machined from the specific alloys and joined using 17 metric tons and 10 metric tons, respectively. Fig. 13 shows actual experimental results for the two permutations. It is observed that the fins are curved as predicted by the model but there is a slight shift of the upper plate with respect to the lower plate. The predicted deformation angle for M-Cu1 was 23.85°, experimental was 16°. For M-Al, predicted deformation angle was 25.16°, experimental –17.5°.

The microstructures show that the copper joint shows some incomplete contact of teeth at the bottom of the lower plate. The aluminum joint shows incomplete contact in both plates coupled with larger tooth/groove gap, as both of these effects were predicted by the computer simulation. Despite these small differences, the model is fairly accurate for the assessment of the various DMT geometries and their effect on joint geometry. Large scale processing of DMT electrical joints is possible; it has the potential to fabricate several joints per minute. We have explored the opportunity to develop an automated DMT line for electrical joints in busbars. However, more cost effective technologies, such as TIG welding [11], or friction stir welding [12], are more attractive.

IV. Conclusion

Using ANSYS 11 Classic software, we developed a fairly accurate model that is capable of predicting the deformation that occurs when joining DMT profiles to fabricate electrical joints. The model provided insight into filling DMT grooves, quantifying tooth interlocking, and determining deformation angle, all being necessary for a reliable electrical joint. The model results showed that the preferred tooth orientation is 90° to the plate surface. For copper joints, the slenderness ratio was determined to be the most important parameter in the design of the DMT joints as it is critical to joint interlocking and gap filling. For aluminum, in addition to the slenderness ratio, the gap between the mating teeth is also critical due to decreased interlocking and spring-back. Aluminum joints were anticipated to provide a less desirable electrical joint compared to copper due to reduced gap filling and material spring-back associated with the lower elastic modulus of aluminum.

Acknowledgment

The authors would like to thank R. Yanniello, Eaton Electrical Sector, Avery Creek, NC, for his insightful discussions and guidance throughout this technical work.

References

[1] K. Duane, "Designing welded lap joints," *Weld. Innovat.*, vol. 18, no. 3, pp. 1–3, 2001.

[2] N. H. Faulkner and S. C. Pauline, "Busway busbar with plug-in tabs," U.S. Patent 5 619 014, Apr. 8, 1997.

[3] N. Zoubkov and A. Ovtchinnikov, "Method and apparatus of producing a surface with alternating ridges and depressions," U.S. Patent 5 775 187, Jul. 7, 1998.

[4] R. Kukowski, "MDT - Micro deformation technology," in *Proc. ASME Int. Mech. Eng. Congr. RD&D Expo*, Washington, DC, Nov. 2003, pp. 305–308.

[5] N. N. Zubkov and A. D. Slepcov, "Production of slotted polymer tubes by deformational cutting," *Russian Eng. Res.*, vol. 30, no. 12, pp. 51–53, 2010.

[6] P. Thors and N. Zoubkov, "Tool for making enhanced heat transfer surfaces," U.S. Patent 7 509 828, Mar. 31, 2009.

[7] P. Thors and N. Zoubkov, "Heat transfer tube including enhanced heat transfer surfaces," U.S. Patent 7 311 137, Dec. 25, 2007.

[8] J. L. Rodriguez, E. R. Alvarez, and F. Q. Moreno, "Study of the distribution of tensions in lap joints welded with lateral beads, employing three dimensional finite elements," *Comput. Struct.*, vol. 82, nos. 15–16, pp. 1259–1266, 2004.

[9] R. Bergmann, H. Böhme, H. Löbl, and S. Großmann, "Model to assess the reliability of electrical joints," in *Proc. 18th Int. Conf. Electr. Contacts*, Chicago, IL, 1996, pp. 180–188.

[10] ANSYS. (2009, Apr.). *ANSYS 14.0*, Canonsburg, PA [Online]. Available: http://www.ansys.com

[11] L. P. Connor and R. L. O'Brien, "American Welding Society," in *Welding Handbook*, vol. 2, 8th ed. Miami, FL: AWS, 1991. ch. 4.

[12] T. Santos, R. Miranda, P. Vila, and J. Teixeira, "Modification of electrical conductivity by friction stir processing of aluminum alloys," *Int. J. Adv. Manuf. Technol.*, vol. 57, nos. 5–8, pp. 511–519, Nov. 2011.

Lyudmila Solovyeva received the Masters degree in material science and engineering from Aviation University, Russia, in 1978, and the Bachelors degree in physical metallurgy and heat treatment.

She was with the Materials Department, Kazan Aircraft Engine Building Production Association, as a Principal Engineer, and later, as a Materials Department Manager for almost 20 years. During this period, her major area of expertise was related to turbine blades. She was involved in research and development of special high-temperature and corrosion-resistant diffusion multicomponent coatings for turbine blades, developing gamma-prime criteria in turbine blades to prevent creep, and developing a technology for reconditioning the microstructures of super alloy turbine blades. In the past 10 years, she was involved in the development of nickel single crystal for turbine blades. She was engaged in development of new materials for automotive components after the Kazan Engine Building Production Association formed a joint corporation with German bus transmission company "Voit." In 1997, she was with Akebono Engineering Brake System Company, Farmington Hills, MI, engaged in friction material characterization using scanning electron microscopy. In 1998, she joined the General Motors Engineering Center, Pontiac/Wixom, MI, where she was engaged in failure analysis of automotive parts for 3 years. In 2001, she joined the Eaton Corporation Southfield, MI as a Lead Engineer with the Materials, Fluids, and Chemicals Technology Group, Eaton Innovation Center, where she was engaged in research and development of nanocoatings for DOE program, metal matrix composites for automotive components, advanced deicing technology for automotive parts, and deformation machining technology from Russia. She has published more than ten research articles in journals and conferences and filed a U.S. patent application in 2009.

Nikolay Zubkov received the Degree from Bauman Moscow State Technical University (BMSTU), Moscow, Russia, in 1979, the Ph.D. degree in mechanical engineering in 1986, and the Doctor of Science degree in 2002.

He is currently the Laboratory Chief with the R&D Institute of Structural Materials and Technological Processes, BMSTU. He has specialized in machining and manufacturing engineering and is the developer of a new method of machining, deformational cutting. He proposed and justified new methods and devices for obtaining new heat-transfer surfaces, including tube internal enhancement, restoring the original dimensions of worn machine parts by turning, making a capillary porous structures for heat pipes, and making fine filtering meshes from sheets, and slotted adjustable filter pipes surface quenching in lathe machining. He is the Head of the Tool Engineering and Technologies cycle of discipline. He has supervised implementation of more than 70 scientific researches. He has published 90 publications, including 25 inventions, five of which are protected by patents in Europe, the U.S., and other countries.

Dr. Zubkov was the recipient of the Gold Medal from the International Exhibition of Invention and Innovation six times, at Brussels, Geneva, Nuremberg, Seoul, Moscow, and Kuala-Lumpur. He was also the recipient of the Grand Prix and the Cup of Asia for Best Invention on ITEX, Malaysia, in 2010, and the Professor Academic Title in 2008.

Bohdan Lisowsky completed the initial formal technical training in casting technology in Poland. He received the Bachelors and Masters degrees in metallurgical engineering from Wayne State University, Detroit, MI, in 1964 and 1966, respectively.

He joined the Engineering and Research Center, Eaton Corporation, Southfield, MI, where he was involved in development of engine valve alloys for unleaded fuels, after a short work assignment with Argonne National Laboratory, Lemont, IL, where he was involved in developing a mercury amalgamation process to detect oxygen content in liquid sodium for atomic reactors. During his 43 year career at Eaton, he conducted specialized materials testing and developed critical metallic and nonmetallic materials for engine valves, air bags, composite leaf springs, reaction-bonded silicon nitrides, and carbon-carbon friction materials. He has developed associated processes, specifications, and supply sources. He is the Chief Engineer and the Director of the Materials Engineering Groups in Southfield and Milwaukee in the developments of a variety of products, materials, and processes for all five of Eaton's market segments: aerospace, automotive, electrical, hydraulics, and truck. He has established an advanced coatings capability with the Innovation Center, Eaton, which led to obtaining a nanocoatings DOE contract. He secured or played a key role in three DOE contracts and was the Principal Investigator on a program to improve truck driveline efficiency working with Caterpillar, Peoria, IL, Northwestern University, Evanston, IL, and Argonne National Laboratory. He holds 17 U.S. patents and 42 foreign patents in Canada, Europe, Turkey, and Japan. In 2004, he was selected as one of five inaugural engineers of the year among engineers of Eaton for his work on carbon-carbon composite friction materials for truck transmissions. Currently, although retired in 2007, he has been a Consultant for Eaton's Innovation Center and the Vehicle Business Group.

Mr. Lisowsky was elected as a fellow of the ASM International and the Professional Materials and Metallurgical Society in 1993.

Alaa Elmoursi received the Ph.D. degree in electrical engineering from the University of Western Ontario, London, ON, Canada, in 1985.

He worked with the General Motors Research Laboratory, Warren, MI, for 14 years, where he was engaged in basic and applied research on electrostatic painting of liquids and powders, conductive plastic surfaces, plasma source ion implantation, DLC, and vacuum-based thin-film coating technologies. In 1991, he joined Delphi Research Laboratory, San Diego, CA, and was involved in research and development in thermal spray and cold spray coatings for numerous applications related to automotive components. At Delphi, he was the Chief Scientist for Delphi Thermal Division, a Group Leader for Coating Materials, and the Manager for Advanced Manufacturing and Material Processing. In 2007, he joined Eaton Corporation Southfield, MI as a Principal Engineer. He was the Principal Investigator for DOE program on nanocoatings and the Program Manager for Smart Materials. He is currently the Technology Manager with the Materials, Fluids and Chemicals Technology Group, Eaton Innovation Center. He has published over 50 research articles in referred journals and conferences and holds over ten U.S. and foreign patents. He has given many invited talks in his fields of expertise.